

An absence of structural changes in the proximal femur with osteoporosis

Satoru Saitoh, M.D.¹, Yukio Nakatsuchi, M.D.¹, Loren Latta, Ph.D.², Edward Milne, B.Sci.²

¹ Department of Orthopaedics, Shinshu University School of Medicine, Matsumoto City, Japan

² University of Miami's Biomechanical Laboratory at Mt. Sinai Medical Center, Miami Beach, Florida, USA

Abstract. The hypothesis that osteoporosis occurs not as a preferential loss of the tensile trabeculae but as a general loss of bone was tested by using bone mineral densitometry and an indentation test on dissected proximal femora. As osteoporosis advanced a significantly correlated decrease was found in both bone mineral density and mechanical properties between the principal compressive and tensile trabeculae. The decrease correlated with a decrease in the Singh index. These findings led to the conclusion that a sequential bone loss from the tensile trabeculae to the compressive ones did not occur as Singh reported, but instead a generalized loss of bone mineral in both the tensile and compressive trabeculae supervened. The structural changes, on which the grading system by Singh was based, were not observed in the proximal femur affected by osteoporosis.

Key words: Osteoporosis – Proximal femur – Singh index – Structural change – Bone mineral density – Indentation test

To evaluate osteoporosis of the proximal femur the Singh index has become popular not only because it is a simple method using a plain radiograph but also because it is supposed to provide quantitative information about osteoporosis in that region. This method depends on the hypothesis that there is a preferential bone loss first in the tensile trabeculae and then in the compressive trabeculae of the proximal femur as osteoporosis advances. For this reason the Singh system is considered to be unaffected by such factors as the overlying soft tissue or exposure factors of radiographs [16].

It is not easy, however, to assign an "adequate" Singh index to each femur based on only its trabecular pattern, since it is hard to detect whether a particular

trabecula has disappeared or has simply become thinner and less conspicuous. One can often observe an attenuated but distinctive primary tensile trabecula as well as the compressive trabecula in an apparently very osteoporotic bone. Wicks found the index unsuitable for predicting the true density of bone in the femoral head [19]. Smith et al. [17] reported wide interobserver variation in determining the Singh index. There still remain controversies over whether a preferential loss or a general loss occurs in osteoporosis of the proximal femur [7, 18].

Our hypothesis is that there is no structural change as proposed by Singh but a general loss of bone in the osteoporotic proximal femur. This hypothesis was examined with an indentation test and bone densitometry.

Materials and methods

One hundred ninety proximal femora from 122 embalmed cadavers were generously provided by the Department of Anatomy at the University of Miami. The age range was from 60 to 101 years (average 80.0 years). There were 42 males, 56 females, and 24 cadavers of unknown gender. Soft tissue was removed as cleanly as possible and the bones were kept in air-tight bags at 4° C before and during the study. The anteroposterior (AP) diameter of the femoral head was measured in a position without anteversion of the head.

Standard AP radiographs of each bone were taken using constant exposure factors of 44 kV, 20 mAs with a film-focus distance of 90 cm. Singh indices of the trabecular pattern of the proximal femur were assigned to each bone independently by three experienced examiners (S.S., E.M., L.L.) and were finalized after discussion.

The bone mineral density (BMD) of 187 proximal femora was measured with dual photon absorptiometry (DPA) utilizing a commercially available bone densitometer system (model DP3, Lunar Radiation Corporation, Madison). Soft tissue was simulated by placing a 2-in. (5-cm)-high Plexiglas sheet beneath the bones. Scanning was performed without anteversion of the femoral head. The shaft of each femur was raised a little so that the head and the posterior intertrochanteric crest were stable on the flat surface of the Plexiglas. The bone mineral density (BMD) of the head, neck, trochanter, and three 1-cm-thick sections was measured in the proximal femur using the regions of interest (ROIs) shown in Fig. 1.

Correspondence to: Satoru Saitoh, M.D., Department of Orthopaedics, Shinshu University School of Medicine, Asahi 3-1-1, Matsumoto City 390, Japan

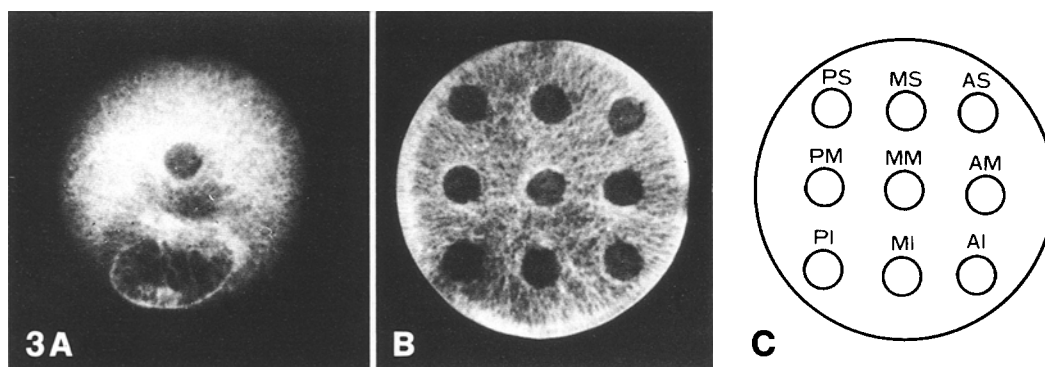
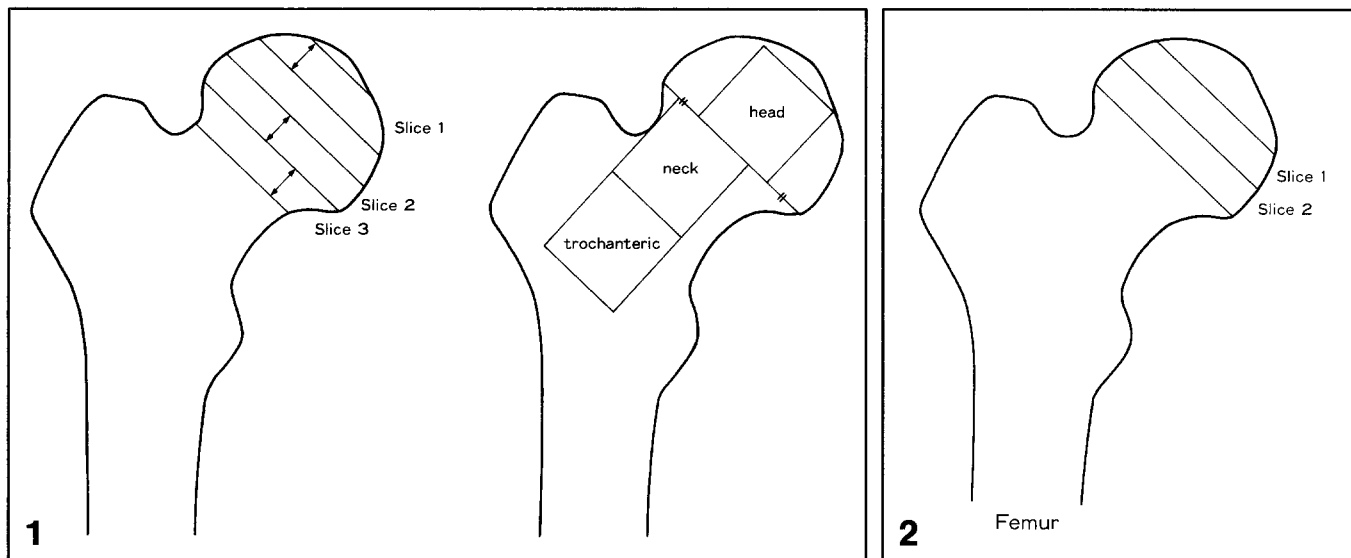


Fig. 1. Regions of interest (ROIs) in the proximal femur. The length of the base of the head was measured on the dual photon absorptiometry (DPA) image and a square with side length of half that length was centered on the base of the head as the ROI for the head. The ROI for the neck is created by turning the ROI of the head round on the base of the head and moving it to the uppermost margin of the neck. That for the trochanter is a reflection of the ROI of the neck but on the lateral side of the ROI of the neck. The ROI for slice 1 is 1 cm high and is located at the top of the head parallel to its base. Those for slices 2 and 3 are also 1 cm thick and are on the base of the head respectively proximal and distal to it (right part reproduced with permission from Mosby-Yearbook [20])

Fig. 2. Bone sections for the indentation test. Slice 2 is a 1-cm-high bone section at the base of the head. Slice 1 is another 1-cm-thick bone section proximal to slice 2. Slice 1 is not located at the top of the head (reproduced with permission [20])

Fig. 3A–C. Marks for indentation test on bone slices. **A** Slice 1; **B** Slice 2; **C** abbreviated name for each indentation point. *AS*, Anterosuperior; *MS*, midsuperior; *PS*, posterosuperior; *AM*, anteromiddle; *MM*, midmiddle; *PM*, postermiddle; *AI*, anteroinferior; *MI*, midinferior; *PI*, posteroinferior (reproduced with permission [20])

An indentation test was performed on the first 86 femora to determine the mechanical strength of the cancellous bone of the head. One-centimeter-thick bony sections of slice 1 and 2 were made at the base of the head using a band saw (Fig. 2). Each section was marked with ink to produce a 10 × 10 mm grid and the indentation test was performed at every crossing point of the grid. The number of indentation points on slice 2 was usually nine, but more than nine points were marked on the larger slice 2. One to three points were marked on slice 1 (Fig. 3).

The indentation test was conducted with an electrohydraulic stress system (model 810, MTS system) and a cylindrical indenter 5 mm in diameter. Each bone section was placed flat on a rigid metal platform with the proximal cut surface facing upwards. The indenter was applied in a perpendicular fashion to each marked point from the top toward the base of the head. The stage on which the bone sections rested was raised at a constant rate of 0.04 mm/s until the indenter hit the surface of the platform and gave a sharp continuous rise in the load-displacement curve.

With each load-displacement curve, the energy required to indent the first 5 mm was calculated from the area between the curve and the baseline (“E” in Fig. 4). The peak value (“P” in Fig. 4) was also determined as the maximum resistant force during the first 5 mm displacement (50% strain of a 10-mm-thick bone section).

The values obtained from the peripheral indentation points were averaged to obtain values of nine standardized points when more than nine indentations were performed. Subsequently, four parameters were calculated from the energy (E) and the peak value (P) of each indentation point to represent the mechanical properties of each section: E_{avg} , the average amount of energy required to indent 5 mm at each indentation point on a bone section; E_{max} , the maximum energy of all of the indentation points on a section; P_{avg} , the average of the peak values in a section; P_{max} , the maximum of the peak values of all indentation points on a section.

Two-way ANOVA analyses were performed in two gender groups and four age groups (group 1: 60–69 years; group 2: 70–79

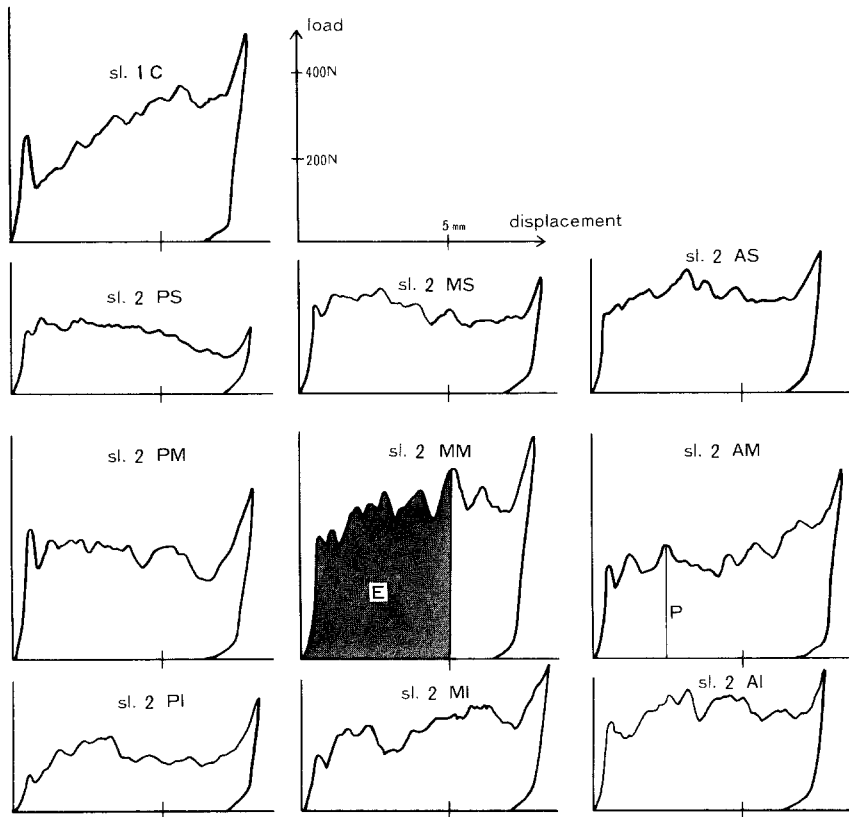


Fig. 4. Load-displacement curves obtained from the indentation test on a femoral head shown in Fig. 3 (from a 76-year-old woman). *sl. 1 C*, center of slice 1; *sl. 2*, slice 2. The location of each indentation point on slice 2 is shown in Fig. 3

years; group 3:80–89 years; group 4:90–99 years) to see if there would be an age-related or gender-related decrease in BMD and in the mechanical properties of the proximal femur. The data were analyzed in three age groups in eight analyses because of data shortage in females from 60 to 69 years old.

With one-way ANOVA analyses, the relation between the decrease in Singh index and that in the BMD and mechanical properties was studied. Special attention was paid as to whether the BMD and mechanical properties of the principal compressive trabeculae decreased synchronously with a decrease in the Singh index and whether those of the principal compressive trabeculae would decrease together with those of the principal tensile ones.

Results

Among the bones harvested, three femoral heads showed slight to moderate osteoarthritis of their articular cartilage. All bones were, however, utilized for analyses since these degenerative changes were generally mild. The mean AP diameter of the femoral head was 4.74 (SD 0.36) cm.

The dual photon absorptiometry image of the proximal femur revealed that the area just proximal to the

crossing point of the principal compressive and principal tensile trabeculae had the highest BMD (Fig. 5). The BMD of the neck and trochanter was not available in eight proximal femora because of the osteotomy at the neck. In one femur the BMD of the trochanter was not obtained since experimental intramedullary reaming had been performed prior to DPA scannings. The BMD of the head was higher than that of the neck or trochanter and the BMD of slice 2 was significantly higher than that of slices 1 or 3 (Table 1, $p < 0.01$, paired *t*-test).

Table 1. Measurement of the bone mineral density (BMD; $g/cm^2 \pm SD$)

Head	0.937 ± 0.275 ($n=187$)
Neck	0.528 ± 0.177 ($n=179$)
Trochanter	0.612 ± 0.218 ($n=178$)
Slice 1	0.666 ± 0.223 ($n=187$)
Slice 2	0.864 ± 0.239 ($n=187$)
Slice 3	0.677 ± 0.202 ($n=187$)

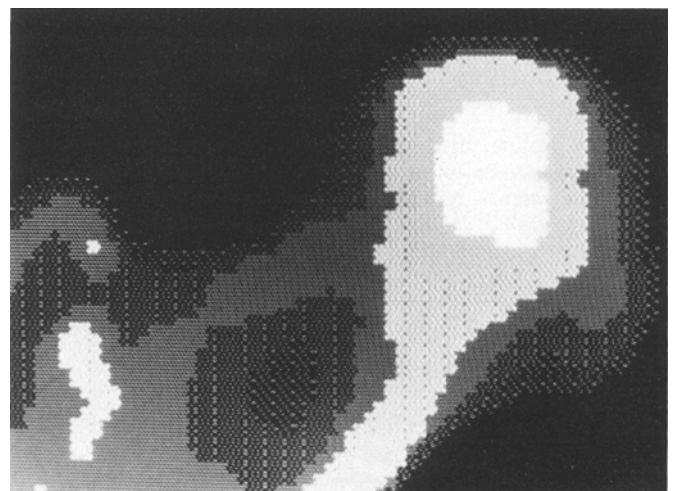


Fig. 5. A DPA image of a femoral head. The area of the highest bone mineral density is located just proximal to the crossing point of the principal compressive and the principal tensile trabeculae

Table 2. Correlation analyses (*r*) on BMD measurements

	Head	Neck	Trochanter	Slice 1	Slice 2	Slice 3
Head	—	0.842974	0.859954	0.929140	0.972326	0.883716
Neck	<i>n</i> =179	—	0.927196	0.782996	0.833893	0.919976
Trochanter	<i>n</i> =178	<i>n</i> =178	—	0.794485	0.843917	0.884136
Slice 1	<i>n</i> =187	<i>n</i> =179	<i>n</i> =178	—	0.909722	0.837245
Slice 2	<i>n</i> =187	<i>n</i> =179	<i>n</i> =178	<i>n</i> =187	—	0.905642
Slice 3	<i>n</i> =187	<i>n</i> =179	<i>n</i> =178	<i>n</i> =187	<i>n</i> =187	—

Table 3. Energy and peak value of each indentation point (data on slice 2 from [20] with permission)

		Anterior	Middle	Posterior
<i>Energy (J ± SD)</i>				
Superior	slice 1	—	1.761 ± 0.901 (<i>n</i> = 64)	—
	slice 2	1.312 ± 0.591 (<i>n</i> = 86)	1.502 ± 0.698 (<i>n</i> = 86)	1.252 ± 0.710 (<i>n</i> = 86)
Middle	slice 1	—	0.858 ± 0.582 (<i>n</i> = 55)	—
	slice 2	1.620 ± 0.700 (<i>n</i> = 86)	2.570 ± 1.056 (<i>n</i> = 86)	1.523 ± 0.656 (<i>n</i> = 86)
Inferior	slice 1	—	0.546 ± 0.274 (<i>n</i> = 18)	—
	slice 2	0.767 ± 0.379 (<i>n</i> = 86)	0.620 ± 0.300 (<i>n</i> = 86)	0.687 ± 0.467 (<i>n</i> = 86)
Slice 1 energy	superior > **middle > **inferior			
Slice 2 energy	MM > **AM > *PM, ^{ns} MS > **AS, ^{ns} PS > **AI > *PI, ^{ns} MI			
<i>Peak value (N ± SD)</i>				
Superior	slice 1	—	494.8 ± 242.9 (<i>n</i> = 64)	—
	slice 2	368.1 ± 169.7 (<i>n</i> = 86)	427.4 ± 199.3 (<i>n</i> = 86)	338.9 ± 188.7 (<i>n</i> = 86)
Middle	slice 1	—	261.0 ± 169.7 (<i>n</i> = 55)	—
	slice 2	491.2 ± 206.7 (<i>n</i> = 86)	804.0 ± 315.5 (<i>n</i> = 86)	443.6 ± 190.3 (<i>n</i> = 86)
Inferior	slice 1	—	169.2 ± 86.3 (<i>n</i> = 18)	—
	slice 2	231.8 ± 112.4 (<i>n</i> = 86)	189.9 ± 84.6 (<i>n</i> = 86)	201.2 ± 131.1 (<i>n</i> = 86)
Slice 1 peak value	superior > **middle > **inferior			
Slice 2 peak value	MM > **AM > **PM, ^{ns} MS > **AS > *PS > **AI > **PI, ^{ns} MI			

^{ns}, not significant; * *p* < 0.05; ** *p* < 0.01; *** *p* < 0.001

AS, Anterosuperior; MS, midsuperior; PS, posterosuperior

AM, Anteromiddle; MM, midmiddle; PM, posteromiddle

AI, Anteroinferior; MI, midinferior; PI, posteroinferior

Table 4. Energy and peak value of slice 1 and slice 2 (data on slice 2 from [20] with permission)

	Slice 1	Slice 2	Paired <i>t</i> -test	Correlation coefficient (<i>r</i>)
<i>E</i> _{avg} (J)	1.20 ± 0.56 (<i>n</i> = 64)	1.32 ± 0.48 (<i>n</i> = 86)	ns	0.813881 (<i>n</i> = 64)***
<i>E</i> _{max} (J)	1.78 ± 0.91 (<i>n</i> = 64)	2.61 ± 1.04 (<i>n</i> = 86)	**	0.775917 (<i>n</i> = 64)***
<i>P</i> _{avg} (N)	349.2 ± 158.0 (<i>n</i> = 64)	388.4 ± 142.4 (<i>n</i> = 86)	*	0.780970 (<i>n</i> = 64)***
<i>P</i> _{max} (N)	502.9 ± 245.7 (<i>n</i> = 64)	805.2 ± 314.4 (<i>n</i> = 86)	**	0.758748 (<i>n</i> = 64)***

*E*_{avg}, Average energy of all the indentation points on a slice,

*E*_{max}, Maximum energy among the indentation points on a slice,

*P*_{avg}, Average peak value of all the indentation points on a slice,

*P*_{max}, Maximum peak value of all the indentation points on a slice

The BMD of the head, neck, trochanter, slices 1, 2, and 3 correlated significantly with one another (Table 2, *p* < 0.001).

The energy and peak values were highest in the center among nine standardized points on slice 2 and highest in the superior part of slice 1 (Table 3). Slice 2 proved to have higher *E*_{max}, *P*_{avg}, and *P*_{max} than slice 1. *E*_{avg}, *E*_{max}, *P*_{avg}, and *P*_{max} of slice 1 decreased along with those of slice 2 (Table 4). Both the energy (*E*) and peak value

(*P*) of all the indentation points on slice 2 correlated significantly with each other except between the posterosuperior and posteroinferior regions.

The BMD of the head or that of slice 2 correlated better with the *E*_{avg} of slice 2 than the age or the Singh index. The normalized BMD of the head or that of slice 2 (the BMD divided by the AP diameter of the corresponding head) correlated even better with the *E*_{avg} of slice 2 than the BMD itself (Table 5).

Table 5. Results of the correlation analysis

E_{avg} of slice 2	vs	age	$r = -0.451816$	$n = 85^{***}$
E_{avg} of slice 2	vs	BMD of the head	$r = +0.891201$	$n = 86^{***}$
E_{avg} of slice 2	vs	BMD of the head/AP diameter	$r = +0.914702$	$n = 86^{***}$
E_{avg} of slice 2	vs	BMD of slice 2	$r = +0.888703$	$n = 85^{***}$
E_{avg} of slice 2	vs	BMD of slice 2/AP diameter	$r = +0.899492$	$n = 85^{***}$
E_{avg} of slice 2	vs	Singh index	$r = +0.613381$	$n = 86^{***}$

Table 6. Correlation analysis and the one-way ANOVA^a regarding the Singh index

		Correlation coefficient	One-way ANOVA
Singh index vs femoral head BMD		0.691775 ($n = 187$) ^{***}	**
vs head BMD/AP diameter		0.637027 ($n = 187$) ^{***}	**
vs neck BMD		0.758972 ($n = 179$) ^{***}	**
vs trochanter BMD		0.784229 ($n = 178$) ^{***}	**
vs slice 1 BMD		0.652122 ($n = 187$) ^{***}	**
vs slice 2 BMD		0.689076 ($n = 187$) ^{***}	**
vs slice 3 BMD		0.733048 ($n = 187$) ^{***}	**
vs age		-0.376517 ($n = 165$) ^{***}	** (6 Singh index groups)
vs E_{max} of slice 1		0.534534 ($n = 64$) ^{***}	**
vs E_{avg} of slice 1		0.478119 ($n = 64$) ^{***}	**
vs P_{max} of slice 1		0.55457 ($n = 64$) ^{***}	**
vs P_{avg} of slice 1		0.468406 ($n = 64$) ^{***}	**
vs E_{max} of slice 2		0.61702 ($n = 86$) ^{***}	**
vs E_{avg} of slice 2		0.613381 ($n = 86$) ^{***}	**
vs P_{max} of slice 2		0.605374 ($n = 86$) ^{***}	**
vs P_{avg} of slice 2		0.608489 ($n = 86$) ^{***}	**
Energy of slice 1	superior	0.513593 ($n = 64$) ^{***}	**
	middle	0.366346 ($n = 55$) ^{**}	*
	inferior	0.212256 ($n = 18$) ns	ns
Energy of slice 2	AS	0.480507 ($n = 86$) ^{***}	**
	MS	0.42853 ($n = 86$) ^{***}	**
	PS	0.242527 ($n = 86$) [*]	*
	AM	0.510852 ($n = 86$) ^{***}	**
	MM	0.616584 ($n = 86$) ^{***}	**
	PM	0.509244 ($n = 86$) ^{***}	**
	AI	0.47586 ($n = 86$) ^{***}	**
	MI	0.568008 ($n = 86$) ^{***}	**
	PI	0.488882 ($n = 86$) ^{***}	**
Peak value of slice 1	superior	0.524563 ($n = 64$) ^{***}	**
	middle	0.346561 ($n = 55$) [*]	*
	inferior	0.144831 ($n = 18$) ns	ns
Peak value of slice 2	AS	0.486205 ($n = 86$) ^{***}	**
	MS	0.446727 ($n = 86$) ^{***}	**
	PS	0.253182 ($n = 86$) [*]	*
	AM	0.517009 ($n = 86$) ^{***}	**
	MM	0.605349 ($n = 86$) ^{***}	**
	PM	0.519797 ($n = 86$) ^{***}	**
	AI	0.461832 ($n = 86$) ^{***}	**
	MI	0.559749 ($n = 86$) ^{***}	**
	PI	0.490289 ($n = 86$) ^{***}	**

^a All of 40 one-way ANOVA analyses were performed in five Singh index groups (Singh index grades 1–5) except for one analysis (Singh index vs age) because of data Shortage in Singh index grade 6

Females were more osteoporotic than males in terms of the Singh index, BMD measurements, and indentation test. The Singh index, BMD of the head, neck, trochanter, slices 2 and 3, and the normalized BMD of the head showed an age-related decrease. E_{avg} , P_{avg} , and P_{max} of slice 2 also disclosed an age-related decrease (two-way ANOVA, $p < 0.05$).

The BMD of the head, neck, trochanter, and slice 1, 2, and 3 demonstrated significant positive correlations

with the Singh index. The energy and peak value of each indentation point on slices 1 and 2 as well as E_{avg} , E_{max} , P_{avg} , and P_{max} of slices 1 and 2 correlated similarly with the Singh index (Table 6).

On the other hand, the one-way ANOVA analyses revealed that the BMD and mechanical properties of the proximal femur decreased along the Singh index. The BMD of slice 1 and the energy (E) and peak value (P) of the superior part of slice 1 and slice 2 (AS, MS,

PS), which represented the BMD and mechanical properties respectively of the principal compressive trabeculae, decreased with reduction of the Singh index. The BMD of the head, neck, slice 2, and slice 3, which reflected both the principal compressive and tensile trabeculae, changed with the Singh index. The mechanical properties of the inferior part of slice 2 (AI, MI, PI), which reflected the principal tensile trabeculae, also decreased together with the Singh index (Table 6).

Discussion

While the Singh index has been reported to correlate with the weight-to-volume ratio of the ash of the excised femoral head [5], with the stability of fixation for the femoral neck fracture [13], and with the femoral neck fracture [6], difficulties in assigning the Singh index have also been reported [8].

There should be no troubles in assigning a Singh index if the trabeculae in the proximal femur disappear in a definite sequence [18] and if structural changes rather than quantitative ones occur with advance of osteoporosis as proposed by Singh [16]. Our study was focused on whether there was a Singh index-related decrease in BMD and mechanical properties of the principal compressive and tensile trabeculae, and thus tried to demonstrate no preferential loss in the principal tensile trabeculae but a general bone loss.

It was not possible to measure directly the BMD of the principal compressive trabeculae or that of the principal tensile ones due to the relatively low resolution and the inability of dual photon absorptiometry to differentiate the BMD of the cortical bone from that of the trabecular bone. The BMD of slice 1, however, represents that of the principal compressive trabeculae and the BMD of the head, neck, slice 2, and slice 3 reflects that of both the principal compressive and tensile trabeculae. Since the BMD of all five of these ROIs changed with the Singh index, it may safely be said that the BMD of both the principal compressive and the principal tensile trabeculae changed in proportion with the Singh index. The BMDs of these five ROIs correlated significantly with each other, indicating that the BMD of the principal compressive trabeculae would change with that of the tensile trabeculae.

The superior parts of slice 1 and slice 2 (AS, MS, PS) in the indentation test reflect the mechanical strength of the principal compressive trabeculae and the inferior part of slice 2 represents that of the principal tensile trabeculae. The center of slice 2 represents both the principal compressive and the principal tensile trabeculae. The energy (E) as well as the peak value (P) of all these indentation points changed along with the Singh index. The mechanical properties of both the principal compressive and tensile trabeculae change respectively with the Singh index. In addition, the energy and peak value of the indentation points reflecting the principal compressive trabeculae correlated with those reflecting the principal tensile ones.

It may be concluded that osteoporosis of the proximal femur occurs not as a preferential loss of the tensile trabeculae but as a general bone loss in both the compressive and the tensile trabeculae. Further, the amount of soft tissue surrounding the proximal femur and the exposure condition of radiographs do have an effect on the reading of the femoral trabecular pattern.

Dual photon absorptiometry (DPA) does not provide an absolute measurement of bone mineral content because the amount of bone scanned differs with the size of the skeleton and must be subsequently normalized [14]. Mechanical properties of cancellous bone are thought to be determined by both true BMD and the direction of the trabecular pattern [2]. They should therefore correlate well with the true BMD if the direction of the trabeculae of each bone is identical. Although the direction of the indentation test in our study was not perpendicular to the principal compressive and tensile trabeculae, it may be assumed to be identical since 1-cm-thick slice 2 was taken consistently from the base of the femoral head. The average of the energy absorbed during 50% strain of the nine standardized points on slice 2 (E_{avg}) correlated well with the BMD determined by DPA of the head and slice 2. Moreover, the normalized BMD (the BMD divided by the AP diameter of the head or slice 2) correlated even better with E_{avg} of slice 2 than the BMD of the head or slice 2 itself. BMD measurement using DPA proved to be a better way of determining the mechanical properties of the proximal femur than either age or the Singh index.

As to the data obtained on mechanical properties of the proximal femur, the peak value of the cancellous bone in this study was much lower than the yield strength reported by Brown et al. [2] even if the effect of embalming on the compressive strength reported by McElhaney et al. [11] is taken into consideration. Brown et al. reported the yield strength of the cancellous bone in the center of the femoral head to be as high as 260 MN/m². Since this number corresponds with those reported for the cortical bone [9, 12], it seems high for cancellous bone. Taking the BMD of the proximal femur into consideration, our values appear more reasonable and are similar to those reported for the cancellous bone [3, 4, 9, 10, 15].

Another clinical application of this study may consist in determining the optimal pin placement for the femoral neck fracture. The superior part of slice 1 and the superior to middle part of slice 2 have a higher BMD and higher mechanical strength than the lower part of slice 1 and slice 2. When three parallel screws are inserted into the neck and head as in the study of Van Audekercke et al. [1] for femoral neck fracture, the two proximal screws can supply sufficient compression pressure against the lateral cortex of the proximal femur while the distal one does not. The distal screw is expected to support the strongest part in the head (the center of the head) on the calcar, preventing medial displacement (varus deformity) of the femoral head on the neck. One should aim at the point slightly lower than the center of the head when a large single hip screw is inserted into the head, since one can expect the screw to

supply sufficient compressive force against the fracture line and to support the strong center of the head on the calcar.

Acknowledgements. This work was supported in part by Mt. Sinai Medical Center, Miami Beach. We are very grateful for the generous cooperation of Dr. Janowitz and Mr. Douglas Fuller at the Department of Nuclear Medicine at Mt. Sinai Medical Center.

References

1. Audekercke R van, Martens MM, Mulier JC, Stuyck J (1979) Experimental study on internal fixation of femoral neck fractures. *Clin Orthop* 141:203
2. Brown TD, Ferguson AB Jr (1980) Mechanical property distributions in the cancellous bone of the human proximal femur. *Acta Orthop Scand* 51:429
3. Burstein AH, Reiley DT, Martens M (1976) Aging of bone tissue: mechanical properties. *J Bone Joint Surg [Am]* 58:82
4. Cater DR, Hayes WC (1977) The compressive behavior of bone as a two-phase porous structure. *J Bone Joint Surg [Am]* 59:954
5. Cooper C, Barker DJ, Hall AJ (1986) Evaluation of the Singh index and femoral calcar width as epidemiologic methods for measuring bone mass in the femoral neck. *Clin Radiol* 37:123
6. Horsman A, Nordin BEC, Simpson M, Speed R (1982) Cortical and trabecular bone status in elderly women with femoral neck fracture. *Clin Orthop* 166:143
7. Kawashima T, Uhthoff HK (1989) Pattern of bone loss of the proximal femur. *Transactions of the 35th Annual Meeting, Orthopaedic Research Society*, vol 14, p 458
8. Khairi MRA, Cronin JH, Robb JA, Smith DM, Johnston CC (1976) Femoral trabecular-pattern index and bone mineral content measurement by photon absorption in senile osteoporosis. *J Bone Joint Surg [Am]* 58:221
9. Lereim P (1988) Mechanical properties of cortical and cancellous bone. *Acta Orthop Scand* 59:197
10. Lindahl O (1976) Mechanical properties of dried defatted spongy bone. *Acta Orthop Scand* 47:11
11. McElhaney J, Fogle J, Byars E, Weaver G (1964) Effect of embalming on the mechanical properties of beef bone. *J Appl Physiol* 19:1234
12. Reiley DT, Burstein AH (1974) The mechanical properties of cortical bone. *J Bone Joint Surg [Am]* 56:1001
13. Rubin R, Trent P, Arnold W, Burstein A (1981) Knowles pinning of experimental femoral neck fractures: biomechanical study. *J Trauma* 21:1036
14. Sartoris DJ (1989) Quantitative bone mineral analysis. *Bone and joint imaging*. Saunders, Philadelphia, pp 202–212
15. Schoenfeld CM, Lautenschlager EP, Meyer PR (1974) Mechanical properties of human cancellous bone in the femoral head. *Med Biol Eng* 12:313
16. Singh M, Nagrath AR, Maini PS (1970) Changes in trabecular pattern of the upper end of the femur as an index of osteoporosis. *J Bone Joint Surg [Am]* 52:457
17. Smith MD, Cody DD, Goldstein SA, Matthews LS (1989) Regional bone density of the proximal femur and biomechanical properties. *Transactions of the 35th Annual Meeting, Orthopaedic Research Society*, vol 14, p 105
18. Weissmann BN (1987) Osteoporosis: radiologic and nuclear medicine procedures. *Public Health Rep [Suppl]*:127
19. Wicks M, Garrett R, Vernon-Roberts B, Fassalari N (1982) Absence of metabolic bone disease in the proximal femur in patients with fracture of the femoral neck. *J Bone Joint Surg [Br]* 64:319
20. Saitoh S, et al (1993) Osteoporosis of the proximal humerus: comparison of bone mineral density and mechanical strength with the proximal femur. *J Shoulder Elbow Surg* 2:78–85